

On the effects of angular acceleration in orientation estimation using inertial measurement units

Felix Brändle, David Meister, Marc Seidel, Robin Strässer, Frank Allgöwer

Abstract—Determining the orientation of a rigid body using an inertial measurement unit is a common problem in many engineering applications. However, sensor fusion algorithms suffer from performance loss when other motions besides the gravitational acceleration affect the accelerometer. In this paper, we show that linear accelerations caused by rotational accelerations lead to additional zeros in the linearized transfer functions, which are strongly dependent on the operating point. These zeros lead to non-minimum phase systems, which are known to be challenging to control. In addition, we demonstrate how Mahony and Madgwick filters can mitigate the effects of the additional acceleration, but at the cost of reduced bandwidth. This generates insights into a fundamental problem in estimation, that are transferable to many practical applications.

I. INTRODUCTION

Determining the rotation of a rigid body is a common problem in engineering and finds application in robotics, unmanned vehicles, human motion tracking, and quadcopters [1], [2]. One possibility to estimate the orientation is to use an inertial measurement unit (IMU) consisting of an accelerometer and a gyroscope. If available, an additional magnetometer can also be employed. By designing a sensor fusion algorithm such as the Mahony filter [3], the Madgwick filter [4], or a Kalman filter [1], these measurements can be combined to obtain an accurate estimate of the true orientation. Since the mere integration of the angular velocities measured by the gyroscope is inaccurate due to drift, the accelerometer can be used to improve the estimate of the true orientation. This approach is based on the assumption, that the IMU is at rest, i.e., the only acceleration affecting the sensor is gravity. Since this acceleration is known in magnitude and direction, it is possible to determine the angular displacement of the sensor with respect to a reference frame.

A known challenge is that if additional external accelerations affect the system, the filter performance deteriorates due to the IMU not being at rest. There already exist a vast number of ways to address this issue, such as optimizing over the filter parameters [5], compensating for this acceleration through a model of the application [6], [7], or using an adaptive scheme as in [8]–[11]. Model-based schemes have

F. Allgöwer is thankful that this work was funded by the Ministry of Science, Research and the Arts of the State of Baden-Württemberg (MWK) in the context of the “MobiLab” Project. F. Brändle thanks the International Max Planck Research School for Intelligent Systems (IMPRS-IS) for its support. D. Meister, M. Seidel, R. Strässer thank the Graduate Academy of the SC SimTech for its support.

F. Brändle, D. Meister, M. Seidel, R. Strässer, and F. Allgöwer are with the University of Stuttgart, Institute for Systems Theory and Automatic Control, 70550 Stuttgart, Germany (e-mail: e-scooter@ist.uni-stuttgart.de).

the disadvantage of requiring a model. Hence, off-the-shelf filters cannot be used. Meanwhile, adaptive schemes treat the acceleration disturbance as an external signal independent of the quantities to be estimated. All of these works consider the estimator as an independent element. When the filter is used in a closed loop together with a controller, an independent external disturbance cannot destabilize the system, at least for linear systems and, by extension, nonlinear systems close to an operating point. However, if the accelerometer is not placed at the rotational axis, any angular acceleration also results in a linear acceleration, which depends on the to be estimated angles themselves. This leads to a different dynamical system with different properties, which may cause instabilities.

One such example with angular accelerations is the Cubli [12]. Due to physical limitations, it is impossible to place the IMU exactly on the rotational axis, leading to linear accelerations due to rotational motion. Interestingly, in this example, this acceleration can be compensated for by employing multiple IMUs [12], [13]. However, there is no analysis of the effects of why this compensation is indeed necessary, besides the need to compensate for all accelerations except the gravitational one.

In this work, we investigate the effects of such an additional acceleration caused by rotational motion around a lever arm. As our main contribution, we show that the linear accelerations caused by angular accelerations lead to a qualitative change of the estimation algorithm by adding additional zeros to the transfer function of the filter. In addition, we show how this change can negatively affect feedback systems if not accounted for. Moreover, we investigate how the filter parameters can be used to mitigate the undesired behavior and what trade-off has to be made in suppressing the effects of the angular acceleration. In particular, our analysis offers insights and tuning guidelines for the Mahony and Madgwick filters, which are widely used in practice. Then, we verify the presented investigations on a real system, where we are able to recover and demonstrate the discussed behavior. We expect those insights to be transferable to other practical applications, allowing for an improved estimation using IMUs.

The paper is structured as follows. In Section II, we present a model to represent angular accelerations and provide the corresponding measurement equations of the IMU. Section III analyzes two common filter methods, when they are applied to the presented model to estimate the orientation. Finally, we validate our findings on an autonomous electric scooter (e-scooter) in Section IV [14], before concluding the

paper in Section V.

Notation: We denote the $n \times m$ zero matrix as $0_{n \times m}$, where we omit the indices if the dimensions are clear from context. Moreover, we use $q \in \mathbb{R}^4$ to denote a unit quaternion and $\hat{q} \in \mathbb{R}^4$ for its estimate. In addition, \otimes denotes quaternion multiplication and q^* the conjugate of a quaternion q , cf. [15]. Further, $a \times b$ is the vector product of $a \in \mathbb{R}^3$ and $b \in \mathbb{R}^3$. We write $a_{i:j}$ for the i th to j th component of the vector $a \in \mathbb{R}^n$, where $1 \leq i < j \leq n$. Finally, $\alpha = \text{atan2}(y, x)$ is the angle α between the positive x -axis and the connection from the origin to the point (x, y) in the Cartesian plane, where $-\pi < \alpha \leq \pi$.

II. MODEL

To model the effects of angular motion around a fixed axis on the estimation, we consider a pendulum as illustrated in Fig. 1. The pendulum generalizes many types of rotational motions, which are not centered around the rotational axis, e.g., loops in aerobatics, joint motions in exoskeletons, or curve driving in vehicles [2], [12], such that our results can be easily transferred to different setups. The IMU is placed at a fixed distance l to the point O and rotates with respect to the roll angle φ while pitch θ and yaw ψ are held at zero. Hence, any acceleration in φ causes a linear acceleration that can be measured by the accelerometer of the IMU.

We align the rotation of the pendulum with the roll angle to investigate whether an acceleration in φ influences the pitch and yaw estimation. Note that the same analysis can be performed around an arbitrary axis, except for the yaw component, which cannot be estimated using accelerometers. Reconstruction of the yaw angle requires additional sensors, e.g., a magnetometer, which also provides redundancy for estimating the pitch angle [4]. An investigation including magnetometers is beyond the scope of this paper and is left for future research. The IMU is able to measure the linear acceleration a^K including gravity and the angular velocity ω^K , both expressed in the body fixed coordinate system K , which is rotated with respect to the inertial frame I . This results in the measurement equations

$$a^K = \begin{pmatrix} 0 \\ \sin(\varphi) - \frac{l}{g}\ddot{\varphi} \\ \cos(\varphi) - \frac{l}{g}\dot{\varphi}^2 \end{pmatrix}, \quad \omega^K = \begin{pmatrix} \dot{\varphi} \\ 0 \\ 0 \end{pmatrix}. \quad (1)$$

These acceleration measurements are already expressed in units of standard gravity $[g]$ and we assume that φ is twice differentiable to ensure the existence of $\ddot{\varphi}$. Since the acceleration depends only on the ratio of l and g , we normalize g to 1 in the following. Further, a common assumption in literature is that the IMU is at rest, i.e., $\dot{\varphi} = \ddot{\varphi} = 0$ such that only gravity affects a^K [1], [3], [4]. Hence, it is possible to compute φ by applying a simple trigonometric function to a^K . In the remainder of the paper, we analyze the effects when the IMU is not at rest.

III. FILTER ANALYSIS

Next, we use quaternion-based formulations of the dynamic filters. Using [15], it is possible to transform quater-

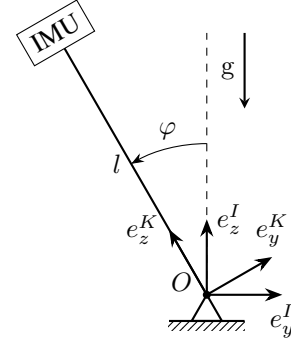


Fig. 1: Pendulum with IMU including gravity g .

nions back and forth between roll, pitch and yaw angles. In particular, we obtain

$$\varphi = \text{atan2}(q_1 q_2 + q_3 q_4, \frac{1}{2} - q_2^2 - q_3^2), \quad (2a)$$

$$\theta = \arcsin(2(q_1 q_3 - q_2 q_4)), \quad (2b)$$

$$\psi = \text{atan2}(q_1 q_4 + q_2 q_3, \frac{1}{2} - q_3^2 - q_4^2) \quad (2c)$$

with $-\pi < \psi \leq \pi$, where

$$q_1 = \cos(\frac{\psi}{2}) \cos(\frac{\theta}{2}) \cos(\frac{\varphi}{2}) + \sin(\frac{\psi}{2}) \sin(\frac{\theta}{2}) \sin(\frac{\varphi}{2}), \quad (3a)$$

$$q_2 = \cos(\frac{\psi}{2}) \cos(\frac{\theta}{2}) \sin(\frac{\varphi}{2}) - \sin(\frac{\psi}{2}) \sin(\frac{\theta}{2}) \cos(\frac{\varphi}{2}), \quad (3b)$$

$$q_3 = \cos(\frac{\psi}{2}) \sin(\frac{\theta}{2}) \cos(\frac{\varphi}{2}) + \sin(\frac{\psi}{2}) \cos(\frac{\theta}{2}) \sin(\frac{\varphi}{2}), \quad (3c)$$

$$q_4 = \sin(\frac{\psi}{2}) \cos(\frac{\theta}{2}) \cos(\frac{\varphi}{2}) - \cos(\frac{\psi}{2}) \sin(\frac{\theta}{2}) \sin(\frac{\varphi}{2}). \quad (3d)$$

A common preprocessing step before applying the measurements to any filter is to first normalize the acceleration measurements [3], [4], [16] as

$$\bar{a}^K = \frac{a^K}{\|a^K\|}. \quad (4)$$

A. One-dimensional case

Before moving to quaternion based formulations for rotation in three dimensions, we consider the one-dimensional case. Later, we show that for quaternion formulations, accelerations in the roll angle do not influence the estimate of the yaw and pitch. In particular, we estimate the angle φ solely based on \bar{a}^K . If the IMU is at rest, i.e., $\dot{\varphi} = \ddot{\varphi} = 0$, it is possible to recover φ exactly as

$$\varphi = \text{atan2}(\bar{a}_2^K, \bar{a}_3^K). \quad (5)$$

To investigate the effects of $\dot{\varphi}$ and $\ddot{\varphi}$, we linearize around an operating point $\varphi = \varphi_{\text{op}}$ with $\dot{\varphi} = \ddot{\varphi} = 0$ and apply the Laplace transform. This leads to the acausal dependence

$$\Delta \hat{\varphi}(s) = (1 - l \cos(\varphi_{\text{op}}) s^2) \Delta \varphi(s) \quad (6)$$

in the frequency domain with zeros $z_{1,2} = \pm \frac{1}{\sqrt{l \cos(\varphi_{\text{op}})}}$ for the deviation from the operating point. Fig. 2 shows the zeros for different operating points. For $\varphi_{\text{op}} = 0$, we obtain two zeros at $\pm \frac{1}{\sqrt{l}}$. This corresponds to one real unstable and one real asymptotically stable zero, leading to deviations from the desired constant transfer function $G_{\Delta\varphi \rightarrow \Delta\hat{\varphi}}(s) \equiv 1$. For low frequencies, the zeros do not affect the estimate. At high

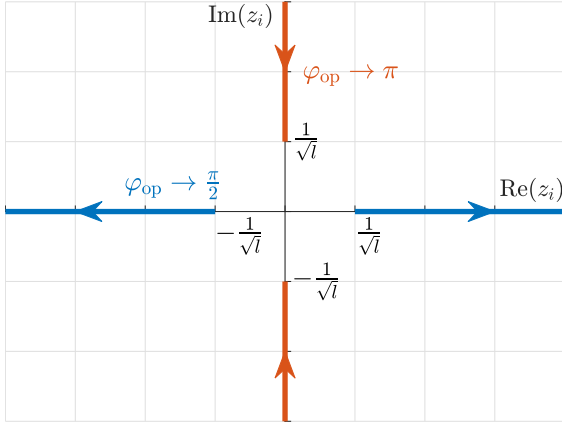


Fig. 2: Location of the zeros for different operating points $\varphi_{\text{op}} \in [0, \pi]$ using (6).

frequencies, however, the zeros result in an amplification of the magnitude. Due to the mirrored zeros, the phase changes of the zeros cancel each other out, such that there is no phase change for all frequencies. As $\varphi_{\text{op}} \rightarrow \frac{\pi}{2}$, the mirrored zeros remain, but move farther away from the origin, resulting in a transfer function closer to 1 for the intermediate frequencies. For $\varphi_{\text{op}} = \frac{\pi}{2}$ the term $l \cos(\varphi_{\text{op}})$ vanishes. Hence, the transfer function becomes exactly $G_{\Delta\varphi \rightarrow \Delta\hat{\varphi}}(s) \equiv 1$ and there is no effect of $\dot{\varphi}$.

For the operating point $\varphi_{\text{op}} \in (\frac{\pi}{2}, \pi]$, there is a qualitative change of the locations of the zeros due to the z -axis of the IMU coordinate system K no longer pointing upwards but downwards. More precisely, the zeros change from being real numbers to being purely imaginary and tend towards $\pm i \frac{1}{\sqrt{l}}$ as $\varphi_{\text{op}} \rightarrow \pi$. As with the upper position $\varphi_{\text{op}} = 0$, the magnitude of high frequency signals is getting amplified due to $\dot{\varphi}$. However, there is a phase change of 180° for frequencies larger than $\frac{1}{\sqrt{l}}$ rad/s, i.e., the sign of the roll angle φ and its estimate $\hat{\varphi}$ differ in sign and magnitude. Further, sinusoids with a frequency $\frac{1}{\sqrt{l}}$ rad/s are getting canceled exactly by the zero, leading to $\hat{\varphi} = 0$. Note that the zeros scale proportionally to $\frac{1}{\sqrt{l}}$. Hence, reducing l also shifts the zeros to higher frequencies, leading to a better estimate in the intermediate frequencies. This behavior is expected, since reducing the distance between the IMU and the rotation axis also decreases the effect of $\dot{\varphi}$.

After establishing the most basic estimation procedure, we extend this to the simultaneous estimation of all angles and incorporating the additional measurements of the gyroscope. To this end, we consider two common filters, the Mahony filter [3] and the Madgwick filter [4], and discuss how the corresponding tuning parameters can be used to improve the rejection of angular accelerations.

B. Mahony filter

The Mahony filter is a particular filter structure based on proportional k_p and integral k_i gains, such that the estimated quaternion \hat{q} tracks the quaternion that rotates the gravitational vector into \bar{a}^K . The resulting filter is described

by the differential equation [3]

$$\begin{pmatrix} \dot{\hat{q}} \\ \dot{\zeta} \end{pmatrix} = \begin{pmatrix} \frac{1}{2} \hat{q} \otimes \begin{pmatrix} 0 \\ \omega^K + \zeta \end{pmatrix} \\ 0_{3 \times 1} \end{pmatrix} + \begin{pmatrix} \frac{1}{2} \hat{q} \otimes \begin{pmatrix} 0 \\ k_p e \end{pmatrix} \\ k_i e \end{pmatrix} \quad (7)$$

with

$$e = \bar{a}^K \times \left(\hat{q}^* \otimes \begin{pmatrix} 0_{3 \times 1} \\ 1 \end{pmatrix} \otimes \hat{q} \right)_{2:4}. \quad (8)$$

Note that this filter can also be interpreted as a disturbance observer [17]. The first summand of (7) represents the nominal prediction for a constant disturbance in ω^K and the second summand characterizes the correction due to the observed measurement error e .

To analyze the estimator, we linearize the filter as before around $\varphi = \varphi_{\text{op}}$ with $\dot{\varphi} = \ddot{\varphi} = 0$ to obtain a linear differential equation with the linearized roll, pitch, and yaw angle of the form

$$\begin{aligned} \Delta \dot{\hat{x}} &= A \Delta \hat{x} + B \Delta \bar{a}^K, \\ \Delta y &= C \Delta \hat{x}. \end{aligned} \quad (9)$$

with $\Delta \hat{x}$ as the stacked linearized estimates $\Delta \hat{q}$ and $\Delta \hat{\zeta}$. Note that other estimation schemes, such as Luenberger observers and, as a special case, the Kalman filter, exhibit the same linear form after linearization, for which k_p and k_i are a particular choice of the observer gains. In the following, we keep k_p and k_i for easier interpretation. System (9) can also be represented via its corresponding transfer function. In particular, after inserting the linearized $\Delta \bar{a}^K$, we get the frequency-domain representation

$$\begin{pmatrix} \Delta \hat{\varphi}(s) \\ \Delta \hat{\theta}(s) \\ \Delta \hat{\psi}(s) \end{pmatrix} = \begin{pmatrix} \frac{k_i + k_p s + (1 - k_i l \cos(\varphi_{\text{op}})) s^2 - k_p l \cos(\varphi_{\text{op}}) s^3}{k_i + k_p s + s^2} \\ 0 \\ 0 \end{pmatrix} \Delta \varphi(s).$$

We observe that the second and third entries are zero and, hence, there are no coupling effects between the roll, pitch, and yaw angles due to a motion in φ . Therefore, we restrict our analysis in the following to the transfer function from $\Delta \varphi$ to $\Delta \hat{\varphi}$. As expected, the poles depend on k_p and k_i , i.e., the gains must be suitably chosen to ensure asymptotic stability. However, the zeros depend on l and the chosen operating point, i.e., they cannot be influenced via the filter gains. Hence, we investigate the effects on the zeros in the Mahony filter setup. Interestingly, for $\varphi_{\text{op}} = \frac{\pi}{2}$ the nominator and the denominator cancel each other out, resulting in the transfer function $G_{\Delta\varphi \rightarrow \Delta\hat{\varphi}}(s) \equiv 1$, which coincides with the results discovered for the one-dimensional case. In particular, $\dot{\varphi}$ has no effect on the estimate around $\varphi_{\text{op}} = \frac{\pi}{2}$. Further, we set $k_i = 0$, i.e., we include no integrator in the filter. This simplification is deployed since integrators are used to compensate for low frequency effects such as a constant bias in the gyroscope. Thus, we can analyze the effects of only one design parameter k_p .

Exploiting the prior discussion, the zeros of the transfer function $G_{\Delta\varphi \rightarrow \Delta\hat{\varphi}}(s)$ are determined by

$$k_p + s - k_p l \cos(\varphi_{\text{op}}) s^2 = 0 \quad (10)$$

with $k_p > 0$ to ensure asymptotic stability. The corresponding zeros can be calculated analytically as

$$z_{1,2} = \frac{-1 \pm \sqrt{1 + 4k_p^2 l \cos(\varphi_{op})}}{2k_p l \cos(\varphi_{op})}. \quad (11)$$

As before, we consider separately two ranges for the operating point. If $\varphi_{op} \in [0, \frac{\pi}{2})$, all zeros are on the real axis without imaginary part. For k_p close to zero, one zero approaches 0 and is canceled by the corresponding pole. The other zero approaches infinity and does not affect the relevant frequencies, leading to a transfer function very close to 1. This is expected, since by setting the gains to zero the filter only integrates the angular velocity, resulting in the true angle. However, the filter is not asymptotically stable, such that constant biases in the gyroscope will also be integrated without any corrections. As k_p approaches infinity, the filter tends aggressively towards the estimate based on the acceleration leading to the zeros $\pm \frac{1}{\sqrt{l \cos(\varphi_{op})}}$. Interestingly, these are identical to the zeros of the one-dimensional case in Section III-A. Note that computing $\arccos(\bar{a}_3^K)$ also returns φ , if the IMU is at rest, while not directly depending on $\dot{\varphi}$. Hence, the fact that the zeros align is a particular property of the atan2.

For $\varphi_{op} \in [0, \frac{\pi}{2})$, there is no qualitative change. In particular, we get one zero with a negative real part and one with a positive real part, but both are shifted further to the right. Hence, the asymptotically stable zero is moved closer to the origin and already affects the estimation for lower velocities. However, the unstable zero is farther away from the zero and hence, affects the estimation only for higher velocities. In contrast, operating points $\varphi_{op} \in (\frac{\pi}{2}, \pi]$ change the qualitative behavior. The zeros are no longer on the imaginary axis, but are shifted to the left half plane. Further, for $k_p \leq \frac{1}{\sqrt{2l \cos(\varphi_{op})}}$, the zeros remain real and for $k_p > \frac{1}{\sqrt{2l \cos(\varphi_{op})}}$ they get an imaginary part approaching $\pm i \frac{1}{\sqrt{l \cos(\varphi_{op})}}$ as in the one-dimensional case. A visualization on how the zeros can be influenced using k_p for $\varphi_{op} = 0$ and $\varphi_{op} = \pi$ is given in Fig. 3. In both cases, k_p must be chosen as a trade-off between fast poles for fast convergence and rejecting the effects of $\dot{\varphi}$ by moving the zeros further away from the imaginary axis.

C. Madgwick filter

In contrast to the Mahony filter, which is designed as a PI-controller, the Madgwick filter can be interpreted as an optimization problem to align the gravitational reference direction with the measured acceleration. More precisely, the Madgwick filter uses a gradient descent algorithm with feedforward compensation for ω^K to minimize the cost function

$$f(\hat{q}, \bar{a}^K) = \left\| \hat{q}^* \otimes \begin{pmatrix} 0_{3 \times 1} \\ 1 \end{pmatrix} \otimes \hat{q} - \begin{pmatrix} 0 \\ \bar{a}^K \end{pmatrix} \right\|^2 \quad (12)$$

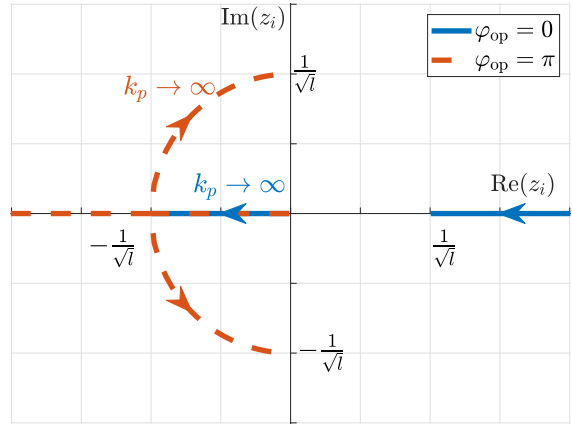


Fig. 3: Location of the zeros for $\varphi_{op} = 0$ and $\varphi_{op} = \pi$ for different k_p .

such that each iteration yields a new quaternion estimate [1], [4]

$$\dot{\hat{q}} = \frac{1}{2} \hat{q} \otimes \begin{pmatrix} 0 \\ \omega^K \end{pmatrix} - \beta \frac{\nabla f(\hat{q}, \bar{a}^K)}{\|\nabla f(\hat{q}, \bar{a}^K)\|} \quad (13)$$

with step size β . In contrast to the Mahony filter, the differential equation (13) cannot be linearized directly due to the normalization of ∇f leading to a discontinuity at $\nabla f = 0$. This non-differentiability is similar to sliding mode observers with sliding surface $\nabla f = 0$. For the following analysis, we first assume β to be sufficiently large to ensure that the filter is tracking $\nabla f = 0$ exactly. To analyze the behavior, we consider the sliding surface and linearize it around an operating point. Without loss of generality, we can fix the yaw $\psi = 0$ and the pitch $\theta = 0$, which leads directly to $q_{op,3} = q_{op,4} = 0$ as operating points. Together with $\bar{a}_1^K = 0$, this yields the linearized representation

$$\nabla f \approx \begin{pmatrix} 4 & 0 & 0 & 0 \\ 0 & 4 & 0 & 0 \\ 0 & 0 & \star & \star \\ 0 & 0 & \star & \star \end{pmatrix} \Delta \hat{q} + \begin{pmatrix} -2q_{op,2} & -2q_{op,1} \\ -2q_{op,1} & 2q_{op,2} \\ 0 & 0 \\ 0 & 0 \end{pmatrix} \Delta \bar{a}_{2:3}^K,$$

where we represent irrelevant entries by \star . In order to investigate the effects of the IMU, we set all initial conditions to zero and deduce $\Delta \hat{q}_3 = \Delta \hat{q}_4 = 0$. Now, we can solve for Δq_1 and Δq_2 on the sliding surface $\nabla f = 0$. Further, when linearizing the transformation from quaternion back to roll, pitch, and yaw around the operating point, it follows from $\frac{\partial \theta}{\partial q_1} = \frac{\partial \theta}{\partial q_2} = \frac{\partial \psi}{\partial q_1} = \frac{\partial \psi}{\partial q_2} = 0$ that the pitch and yaw are independent on the acceleration measurements. Hence, as with the Mahony filter, we deduce that violating the rest condition for one angle does not affect the estimation of the other angles. This can finally be inserted into the linearized equation (2a) for φ such that the angle can be estimated by

$$\Delta \hat{\varphi}(s) = (1 - l \cos(\varphi_{op}) s^2) \Delta \varphi(s). \quad (14)$$

This estimate is equivalent to the one in (6) for the one-dimensional case. Now, we can apply the previous analysis to this sliding surface. As with the Mahony filter, we can use the measurement of the angular velocity to reduce the

effects of $\ddot{\varphi}$. For the simplest case $\beta = 0$, the filter integrates the gyroscope measurements without any error correction. Due to the non-differentiable dynamics, a detailed analysis is not as readily available as for linear systems and the effects of frequency and amplitude cannot be decoupled. For example, the difference between sliding surface and true angle increases for 1) larger $\ddot{\varphi}$, e.g., faster oscillations, and 2) by scaling φ with a constant factor. Due to the normalization, the filter can only move to the sliding surface with a speed of at most β . If the sliding surface changes faster, the filter cannot track it accurately. However, a small β generally leads to a filter which relies more on the integrated gyroscope values, and a larger β yields an estimate that is closer to the sliding surface and may also compensate for the bias in the gyroscope measurements. Hence, the step size β acts as a tuning parameter to trade off fast convergence and rejection of the effects of $\ddot{\varphi}$.

D. Discussion

We emphasize again that the difference between φ and $\hat{\varphi}$ is not caused by an independent, external disturbance. For the linear case and, thus, also for the nonlinear case close to an operating point, such a signal cannot change the stability properties in a feedback system. In particular, $\ddot{\varphi}$ cannot be interpreted as an independent, external signal, since $\ddot{\varphi}$ and φ depend on each other. As shown before, this introduces additional zeros to the transfer function of the estimator, which changes the ideal transfer function of the estimator away from 1 for higher frequencies. This validates and explains previous observations in, e.g., [2] that the filters commonly have to be tuned for the corresponding application. More precisely, our analysis uncovers that the behavior can drastically change depending on the operating point.

The zeros of feedback systems can have a significant effect on the closed loop. In particular, the unstable zero around the upper equilibrium of the pendulum leads to non-minimum phase systems. Thus, the controller design becomes challenging and the achievable performance is limited when using the estimate in the controller design [18]–[21]. Asymptotically stable zeros, on the other hand, also degrade the estimate, but they introduce additional phase into the system, which can be used to increase the phase margin and, hence, the robustness. An example of this are lead compensators that employ asymptotically stable zeros due to their phase increase. Note that canceling undesirable zeros is only possible for zeros in the left-half plane by adding a corresponding pole. While canceling unstable zeros leads to a loss of internal stability and should be avoided, canceling asymptotically stable zeros should also be done carefully. Further, adding a slow pole for cancellation can help with the effects of $\ddot{\varphi}$, but may decrease the overall estimator performance. We emphasize that the location of zeros cannot be modified by feedback.

Our analysis suggests several possibilities to address these issues. First, when designing the system, the IMU should be placed close to the rotational axis. This reduces l and

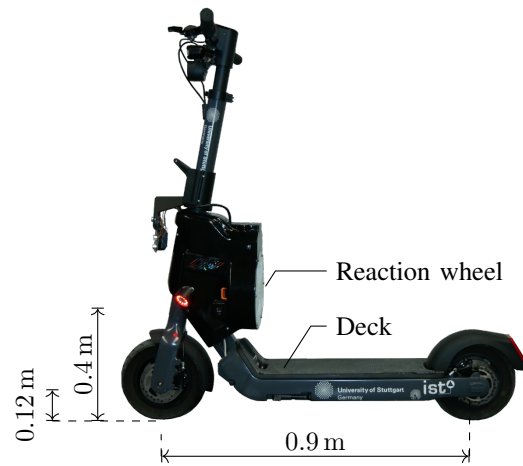


Fig. 4: Autonomous e-scooter [22].

moves the zeros to a higher frequency range, such that for intermediate frequencies the estimate remains accurate. Secondly, the filter parameters can be chosen to rely less on the accelerometer and more on the gyroscope. For the Mahony and the Madgwick filters, this can be done by reducing the corresponding gains k_p and β , but at the cost of reduced bandwidth. Moreover, a model can be used to account for $\ddot{\varphi}$, e.g., [12] uses multiple IMUs with known kinematics to eliminate $\ddot{\varphi}$ from the measurements. Further, the numerical differentiation of the gyroscope measurement can be used to calculate $\ddot{\varphi}$, and if l is known, it is possible to compensate for the angular acceleration. However, this requires a sufficiently accurate gyroscope. Lastly, when designing a controller, the filter dynamics must be taken into account to avoid loss of stability. Our analysis clearly shows that an independent design of estimator and controller, as allowed by the separation principle for linear systems, is not applicable for the considered setup.

IV. EXPERIMENT

In this section, we validate the theoretical result presented in the previous section on a real system and show that the effects of the rotational orientation can play a significant role in feedback systems. To this end, we consider an autonomous e-scooter illustrated in Fig. 4 [14], [23]. The e-scooter is equipped with a reaction wheel to stabilize it around the upper equilibrium to enable autonomous driving. To avoid falling over, the e-scooter needs to be able to measure or at least estimate the current roll angle φ . This estimate is fed into a cascaded PI- and PD-controller, which calculates a desired motor current to simultaneously keep the e-scooter from falling over and keep the reaction wheel speed low [24]. The e-scooter is controlled by two *VESC 6 MK V* motor controllers. Each *VESC 6 MK V* has a built-in *BMI 160* IMU with gyroscope and accelerometer. The first one is placed behind the reaction wheel at height $l = 0.4$ m and actuates the reaction wheel itself. The second motor controller is located in the deck at height $l = 0.12$ m and ensures that

a desired speed is maintained. For comparison, the center of gravity is in between at a height of 0.17 m.

To investigate the effects of the IMU, we let the scooter stabilize the upper equilibrium at standstill without any external excitation. For the first 10 s we use the estimated roll angle of the lower IMU. After 10 s the controller switches to the estimate of the upper IMU and switches back after another 10 s. As an estimation algorithm, we compare the Mahony filter for different values of k_p and k_i . A specific characteristic of the chosen controller structure is that by controlling the reaction wheel velocity to be small, while also including only a proportional part for the control of φ , the e-scooter automatically converges to the equilibrium with $\dot{\varphi} = 0 \frac{\circ}{s}$ and no reaction wheel velocity. However, due to minor calibration mismatches in the accelerometer and a slight imbalance of the e-scooter, this equilibrium is not exactly zero, but is about $\pm 0.3^\circ$ depending on the IMU. For visualization purposes, we center the following plots around 0° and indicate the mismatch by using Δ as the difference to the upper equilibrium. Further, we only show \bar{a}_2^K , since this is the only measurement depending on $\dot{\varphi}$. Fig. 5 shows the resulting closed-loop behavior for $k_p = 10$ and $k_i = 1$. For the first 10 s the lower IMU is used and the e-scooter remains at the equilibrium. However, when switching to the upper IMU, the slight mismatch in the calibration of the accelerometers leads to a small excitation of the system. As indicated by the measurements of $\dot{\varphi}$, this results in fast oscillations in the roll angle, which do not vanish over time. This oscillation also leads to significantly varying acceleration measurements Δa_2^K and consequently to the varying estimated roll $\Delta \hat{\varphi}$. As shown in Section III, the lower IMU is less affected by this effect. When switching back to the lower IMU in the deck, the oscillations quickly vanish and the acceleration measurements and estimates $\Delta \hat{\varphi}$ resemble each other again. This highlights the effect of taking feedback into account. When the lower IMU is used for control, the estimates of the upper and the lower IMU behave similarly. In this case, the upper IMU operates in open loop and has no effect on the system. However, when using the upper IMU, the non-minimum phase behavior is more prevalent and the estimation error is amplified in the closed loop.

To illustrate the effects of different filter parameters, we reduce k_p to $k_p = 2.2$ in Fig. 6. For this parameter set, there are no oscillations when employing the upper IMU in the control loop. The lower value of k_p reduces the effect of the accelerometer, such that the filter relies more on the integrated measurements of the gyroscope and the corresponding zeros of the filter are farther away from the controller bandwidth.

Fig. 7 and Fig. 8 show the same experiment, but for the Madgwick filter with $\beta = 0.1$ and $\beta = 0.01$ instead. The closed loop shows a similar behavior as for the Mahony filter. Large values of β increase the effects of $\dot{\varphi}$ and result in fast oscillations when the upper IMU is employed in the closed loop. A smaller β attenuates the angular acceleration by relying more on the gyroscope and less on the accelerometer,

but requires a sufficiently accurate gyroscope.

With the conducted experiments we are able to recover the theoretical results of Section III. To further reduce the effects of $\dot{\varphi}$, multiple IMUs can be used [12]. Alternatively, if there are no further sensors available and the existing sensor cannot be placed closer to the rotational axis, one possibility is to jointly design the controller and the filter to directly account for the effects of angular accelerations in the closed loop.

V. OUTLOOK

In this work, we investigated the effects of rotational accelerations on the orientation estimation for different sensor fusion algorithms using an IMU. We showed that this leads to non-minimum phase systems, which are known to be challenging when designing stabilizing feedback laws. Further, we analyzed how common filter methods behave in this case and how appropriate parameter tuning can mitigate these effects. However, mitigation comes at the cost of a reduced filter bandwidth, leading to slower rejection of other disturbances and initial estimation errors. Finally, we validated our theoretical findings on a real system by showing that the performance of the closed loop can deteriorate significantly if the filter is not properly tuned to mitigate angular accelerations. Hence, the controller and filter cannot be designed independently. Moreover, it may be interesting to investigate the effect of additional magnetometer measurements and how different adaptive filtering algorithms behave.

REFERENCES

- [1] S. A. Ludwig and K. D. Burnham, "Comparison of Euler estimate using extended Kalman filter, Madgwick and Mahony on quadcopter flight data," in *Proc. International Conference on Unmanned Aircraft Systems (ICUAS)*, 2018, pp. 1236–1241.
- [2] M. Nazarahari and H. Rouhani, "40 years of sensor fusion for orientation tracking via magnetic and inertial measurement units: Methods, lessons learned, and future challenges," *Information Fusion*, vol. 68, pp. 67–84, 2021.
- [3] R. Mahony, T. Hamel, and J.-M. Pflimlin, "Nonlinear complementary filters on the special orthogonal group," *IEEE Transactions on Automatic Control*, vol. 53, no. 5, pp. 1203–1218, 2008.
- [4] S. O. H. Madgwick, A. J. L. Harrison, and R. Vaidyanathan, "Estimation of IMU and MARG orientation using a gradient descent algorithm," in *Proc. IEEE International Conference on Rehabilitation Robotics*, 2011, pp. 1–7.
- [5] S. Ludwig, *Optimization of Control Parameter for Filter Algorithms for Attitude and Heading Reference Systems*. IEEE Congress on Evolutionary Computation (CEC), 2018.
- [6] H. Ahmed and M. Tahir, "Accurate attitude estimation of a moving land vehicle using low-cost MEMS IMU sensors," *IEEE Transactions on Intelligent Transportation Systems*, vol. 18, no. 7, pp. 1723–1739, 2017.
- [7] E. Biales, P. Urda, and J. L. Escalona, "Track frame approach for heading and attitude estimation in operating railways using on-board MEMS sensor and encoder," *Measurement*, vol. 184, p. 109898, 2021.
- [8] X. Wei, S. Fan, Y. Zhang, W. Gao, F. Shen, X. Ming, and J. Yang, "A robust adaptive error state Kalman filter for MEMS IMU attitude estimation under dynamic acceleration," *Measurement*, vol. 242, p. 116097, 2025.
- [9] B. Candan and H. E. Soken, "Robust attitude estimation using IMU-only measurements," *IEEE Transactions on Instrumentation and Measurement*, vol. 70, pp. 1–9, 2021.

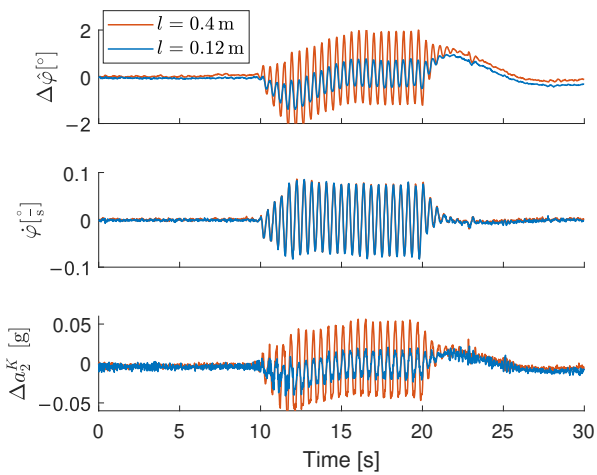


Fig. 5: Closed loop with Mahony filter, $k_p = 10$, $k_i = 1$.

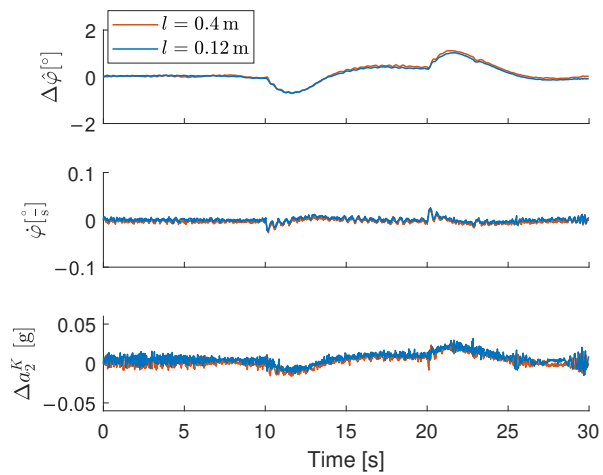


Fig. 6: Closed loop with Mahony filter, $k_p = 2.2$, $k_i = 1$.

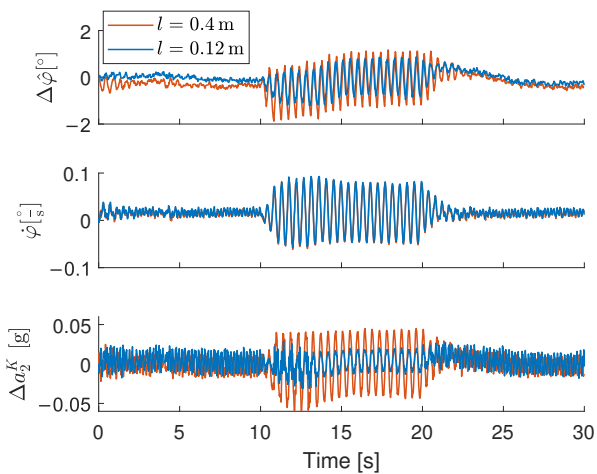


Fig. 7: Closed loop with Madgwick filter, $\beta = 0.1$.

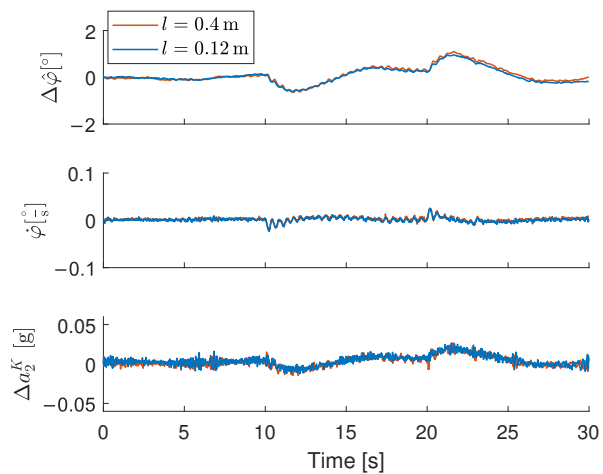


Fig. 8: Closed loop with Madgwick filter, $\beta = 0.01$.

- [10] A. Makni, H. Fourati, and A. Y. Kibangou, "Energy-aware adaptive attitude estimation under external acceleration for pedestrian navigation," *IEEE/ASME Transactions on Mechatronics*, vol. 21, no. 3, pp. 1366–1375, 2016.
- [11] S. Park, J. Park, and C. G. Park, "Adaptive attitude estimation for low-cost MEMS IMU using ellipsoidal method," *IEEE Transactions on Instrumentation and Measurement*, vol. 69, no. 9, pp. 7082–7091, 2020.
- [12] M. Gajamohan, M. Merz, I. Thommen, and R. D'Andrea, "The Cubli: A cube that can jump up and balance," in *Proc. IEEE/RSJ International Conference on Intelligent Robots and Systems*, 2012, pp. 3722–3727.
- [13] S. Trimpe and R. D'Andrea, "Accelerometer-based tilt estimation of a rigid body with only rotational degrees of freedom," in *Proc. IEEE International Conference on Robotics and Automation*, 2010, pp. 2630–2636.
- [14] R. Soloperto, P. Wenzelburger, D. Meister, D. Scheuble, V. S. M. Breidohr, and F. Allgöwer, "A control framework for autonomous e-scooters," *IFAC-PapersOnLine*, vol. 54, no. 2, pp. 252–258, 2021.
- [15] P. Berner, "Orientation, rotation, velocity, and acceleration and the SRM," *SEDRIS Organization. ISO/IEC JTC*, 2007.
- [16] M. Euston, P. Coote, R. Mahony, J. Kim, and T. Hamel, "A complementary filter for attitude estimation of a fixed-wing UAV," in *Proc. IEEE/RSJ International Conference on Intelligent Robots and Systems*, 2008, pp. 340–345.
- [17] B. R. Andrievsky and I. B. Furtat, "Disturbance observers: Methods and applications. i. methods," *Automation and Remote Control*, vol. 81, no. 9, pp. 1563–1610, 2020.
- [18] L. Qiu and E. J. Davison, "Performance limitations of non-minimum phase systems in the servomechanism problem," *Automatica*, vol. 29, no. 2, pp. 337–349, 1993.
- [19] J. Freudenberg and D. Looze, "Right half plane poles and zeros and design tradeoffs in feedback systems," *IEEE Transactions on Automatic Control*, vol. 30, no. 6, pp. 555–565, 1985.
- [20] V. Cheng and C. Desoer, "Limitations on the closed-loop transfer function due to right-half plane transmission zeros of the plant," *IEEE Transactions on Automatic Control*, vol. 25, no. 6, pp. 1218–1220, 1980.
- [21] P. Misra, "On the control of non-minimum phase systems," in *Proc. American Control Conference*, 1989, pp. 1295–1296.
- [22] R. Strässer, M. Seidel, F. Brändle, D. Meister, R. Soloperto, D. H. Ferrer, and F. Allgöwer, "Collision avoidance safety filter for an autonomous e-scooter using ultrasonic sensors," *IFAC-PapersOnLine*, vol. 58, no. 10, pp. 22–28, 2024.
- [23] R. Strässer, F. Brändle, D. Meister, M. Seidel, and F. Allgöwer, "Autonomous e-scooters for sustainable urban mobility: Achievements and insights from an experimental prototype," in *European Robotics Forum*. Springer, 2025, to appear.
- [24] P. Wenzelburger and F. Allgöwer, "A first step towards an autonomously driving e-scooter," *Demonstrator Session 21st IFAC World Congress*, 2020.